JFM RAPIDS
journals.cambridge.org/rapids

Settling regimes of inertial particles in isotropic turbulence

G. H. Good[1,3,4,†], **P. J. Ireland**[1,4]**, G. P. Bewley**[3,4]**, E. Bodenschatz**[1,3,4]**,
L. R. Collins**[1,4] **and Z. Warhaft**[1,2,4]

[1]Sibley School of Mechanical and Aerospace Engineering, Cornell University, Ithaca,
NY 14853, USA

[2]Atkinson Center for a Sustainable Future, Cornell University, Ithaca, NY 14853, USA

[3]Max Planck Institute for Dynamics and Self-Organization, 37077 Göttingen, Germany

[4]International Collaboration for Turbulence Research

We investigate the settling speeds and root mean square (r.m.s.) velocities of inertial particles in isotropic turbulence with gravity using experiments with water droplets in air turbulence from 32 loudspeaker jets and direct numerical simulations (DNS). The dependence on particle inertia, gravity and the scales of both the smallest and largest turbulent eddies is investigated. We isolate the mechanisms of turbulence settling modification and find that the reduced settling speeds of large particles in experiments are due to nonlinear drag effects. We demonstrate using DNS that reduced settling speeds with linear drag (e.g. see Nielsen, *J. Sedim. Petrol.*, vol. 63, 1993, pp. 835–838) only arise in artificial flows that, by design, eliminate preferential sweeping by the eddies. Gravity and inertia both reduce the particle r.m.s. velocities and falling particles are more responsive to vertical than to horizontal fluctuations. The model by Wang & Stock (*J. Atmos. Sci.*, vol. 50, 1993, pp. 1897–1913) captures these trends.

Key words: multiphase and particle-laden flows, particle/fluid flows, turbulent flows

1. Introduction

The behaviour of heavy inertial particles in turbulent flows is relevant for both environmental and engineering problems. Applications include sediment transport in surface water flows, water droplets or aerosols in atmospheric turbulence, volcanic eruptions, dust storms, fluidized beds and soot particle dispersion. Particle settling is an important aspect to each of these, affecting not only the individual particle motions but also the rate of particle collisions. Various investigations have indicated that

† Email address for correspondence: ghg36@cornell.edu

turbulence can either enhance or inhibit settling, and models have been proposed for how this occurs and according to what parameters. Consensus as to the existence of each mechanism in real turbulence is, however, lacking, as is an understanding of their interplay, in part because their dependence upon the governing two-parameter space of the particle inertia and, separately, its weight (or gravity) has not been sufficiently resolved. We aim to address this issue with new experimental measurements of particle settling speeds through controlled turbulence and direct numerical simulations (DNS) over a wide range of conditions.

While weakly inertial particles may become indefinitely trapped in a forced vortex (Tooby, Gerald & John 1977), the transient nature of turbulence gives rise to increased settling speeds for sufficiently small particles. This results from an oversampling of downward-moving flow, e.g. the tendency for inertial particles to circumvent vortex cores towards downwashes (over upwashes). This 'fast-tracking' (or 'preferential sweeping') effect has been observed in DNS of simple flows (Maxey 1987; Dávila & Hunt 2001; Hill 2005) and turbulence (Wang & Maxey 1993; Yang & Lei 1998), and in experiments (Nielsen 1993; Aliseda *et al.* 2002; Yang & Shy 2003, 2005). The effect is strongest for particles that couple best to the smallest eddies – less inertial particles behave like tracers, while the coupling of more inertial particles to larger slower structures is apparently diminished by the smaller vortices. Sufficient fall speeds also prevent particles from side-stepping eddies and fast-tracking; Ghosh *et al.* (2005) argue that fast-tracking vanishes when a particle's stopping distance exceeds its typical path length around even the largest eddies.

If a particle does not oversample the downward flow, it may instead oversample the upward flow. Nielsen (1993) hypothesized that fast-falling particles that bisect both upward- and downward-moving regions of flow require more time to cross the former, a sampling phenomenon he referred to as 'loitering'. The net effect of this delay is expected to be maximum for particles falling at speeds similar to the turbulence root mean square (r.m.s.) velocity (Nielsen 1993; Kawanisi & Shiozaki 2008). Indeed, there is even experimental evidence of a transition to reduced settling speeds where this condition is met (Murray 1970; Nielsen 1993; Yang & Shy 2003; Kawanisi & Shiozaki 2008). However, surprisingly, DNS with a linear drag law cannot capture turbulence-reduced settling speeds; it is only by introducing a nonlinear drag law that DNS yields these speeds (Wang & Maxey 1993; Yang & Lei 1998; Ireland & Collins 2012). In this case, the increase in the drag coefficient with the slip velocity introduces another bias for upward flows that is essential for reduced settling speeds to occur. In all cases, turbulent settling speeds approach still-fluid values for the limits of zero and infinite particle weight or inertia.

The objective of this paper is to study the mechanisms of turbulence settling modification and in particular to determine the extent to which fast-tracking, loitering and nonlinear drag are responsible for the enhancements or reductions in particle settling velocities. The focus of this work is on inertial particles that are much denser than the carrier fluid (e.g. aerosol particles in air). The study is motivated by the bifurcated settling effects observed in the entrainment experiments of Good, Gerashchenko & Warhaft (2012) (in agreement with the findings of Nielsen 1993), but not in the matched DNS of Ireland & Collins (2012) (which instead agreed with Wang & Maxey 1993). (We note that the enhancement regime for small droplets in Good *et al.* (2012) is exaggerated by a weak mean flow.)

2. Methodology

2.1. *Nomenclature and conditions*

We are concerned with the stationary isotropic turbulent flow of a fluid with density ρ, kinematic viscosity ν and velocity $\boldsymbol{u}(\boldsymbol{x}, t)$. The turbulence is parameterized by its r.m.s. velocity u' and energy dissipation rate ϵ. The large scales of the turbulence are represented by the longitudinal integral scale, ℓ, and the large-eddy turnover time, $\tau_\ell \equiv \ell/u'$, while the small scales are described by the Kolmogorov length, time and velocity, $\eta \equiv (\nu^3/\epsilon)^{1/4}$, $\tau_\eta \equiv (\nu/\epsilon)^{1/2}$ and $u_\eta \equiv (\nu\epsilon)^{1/4}$, respectively. We characterize the turbulence using the Taylor-microscale Reynolds number $R_\lambda \equiv (15u'^4/\nu\epsilon)^{1/2}$. In addition to the turbulence parameters, we introduce the gravity constant through the Froude number, defined here as $Fr \equiv a_o^{1/2}(\epsilon^3/\nu)^{1/4}/g$, where $a_o^{1/2}(\epsilon^3/\nu)^{1/4}$ is the fluid acceleration r.m.s. and g is the gravitational acceleration in the *vertical* direction, about which the system is axisymmetric. The coefficient a_o is a weak function of R_λ (Sawford *et al.* 2003).

The flow contains spherical particles of density $\rho_p/\rho \gg 1$, diameter $d < \eta$ and inertial response time $\tau_p \equiv d^2(\rho_p/\rho - 1)/18\nu$. The particles have velocity $\boldsymbol{u_p}$, mean turbulent settling speed W and turbulent r.m.s. velocity $u_p' \equiv [(w_p'^2 + 2v_p'^2)/3]^{1/2}$, where w_p' and v_p' are its vertical and horizontal components, respectively. The still-fluid fall speed is $W_o \equiv \tau_p g/f_D$, where the factor f_D represents the increase in the drag coefficient from the Stokes drag value (for which $f_D = 1$) due to nonlinear drag effects. The dependence of f_D on the particle Reynolds number is given below. We restrict our attention to the case of one-way coupling between the flow and single particles. Physically, this requires the particles to be dilute enough not to interact or modify the turbulence by their collective drag. It also requires them to be smaller than the smallest structures of the flow ($d < \eta$).

A number of dimensionless groups can be formed to describe gravitational settling through turbulence. Gravity and particle inertia provide a two-parameter space and previous work indicates that the scales of both the smallest and largest eddies are consequential. We thus define particle Stokes numbers $St_\eta \equiv \tau_p/\tau_\eta$ and $St_\ell \equiv \tau_p/\tau_\ell$ and settling parameters $Sv_\eta \equiv \tau_p g/u_\eta$ and $Sv_\ell \equiv \tau_p g/u'$. It should be noted that $Fr = a_o^{1/2}St_\eta/Sv_\eta$.

2.2. *Experiment*

Air turbulence was generated at the centre of a one-metre diameter ball via 32 randomly driven loudspeaker jets mounted through its surface (see figure 1). This is an acrylic version of the device used by Chang, Bewley & Bodenschatz (2012), with the jet axes oriented normal to the faces of a truncated icosahedron (soccer ball). The jets are focused by truncated cones, creating a homogeneous isotropic turbulent region approximately 10 cm in size at the centre of the ball.

Water droplets were deposited at the top of the ball by a syringe pump and ultrasonic nozzle (Sono-Tek, Inc.). Two-dimensional measurements were made at the ball centre using a single high-speed camera ($\geqslant$4000 Hz) with shadow imaging (3.2 µm pixel^{-1} resolution, 1.6^2 mm^2 window, as in Bewley, Saw & Bodenschatz 2013) and the depth of field ranging from 2.5 to 3.5 mm for sufficient data rates. Individual droplets were observed for approximately 10 frames on average and their velocities were determined using the particle-tracking algorithm of Kelley & Ouellette (2011). The diameters of the spherical droplets were determined from their images using the major axis of the ellipse with equal second area moments.
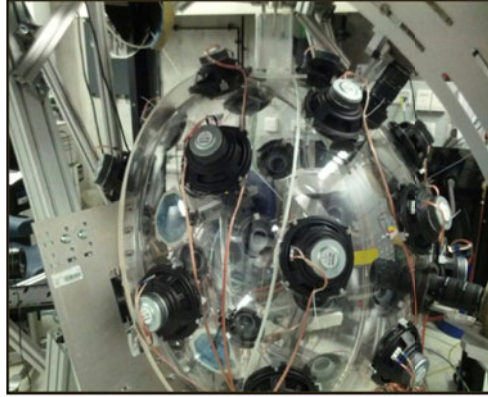
FIGURE 1. The 'soccer ball' apparatus with 32 loudspeaker jets, an ultrasonic nozzle (top) and a high-speed camera (right).

	R_λ	Fr	$a_o^{1/2}$	u'/u_η	ℓ/η	u'	ϵ	ℓ	η
E1	150	0.50(5)	1.70(6)	6.2(2)	97(12)	0.260(5)	0.20(3)	0.035(6)	360×10^{-6}
E2	160	0.9	1.72(5)	6.4(2)	106(13)	0.330(5)	0.46(5)	0.031(4)	290×10^{-6}
E3	176(9)	2.3	1.75(5)	6.7(2)	122(12)	0.47	1.6	0.027(2)	220×10^{-6}
S1	105	—	1.60	5.19	68.1	0.640	0.277	0.458	6.73×10^{-3}
S2	140	—	1.69	6.02	106	0.915	0.267	1.40	13.2×10^{-3}
S3	227	—	1.84	7.65	206	0.915	0.246	1.43	6.94×10^{-3}

TABLE 1. The properties of the experiments (E1, E2 and E3) and the simulations (S1, S2 and S3). The experimental values have standard units. The DNS have arbitrary units and 256^3 (S2) or 512^3 (S1 and S3) grid points; their Froude numbers range from 10^{-3} to infinity ($g = 0$). The Froude numbers for each simulation correspond to a fixed range of Sv_η for each particle Stokes number.

The droplet velocities usually varied by only a few per cent in the measurement volume and the median measured value for each particle was taken for the Eulerian ensemble statistics. The particle volume fraction was approximately 10^{-6} and the energy added to the flow by the particles' collective drag was thus approximately 1 % of ϵ, sufficiently small to not discernably modify the turbulence (Elghobashi & Truesdell 1993; Sundaram & Collins 1999; Bosse & Kleiser 2006). The flow mean and u' velocities were determined from the smallest droplets and ϵ is empirically known from previous 3D tracking measurements (Bewley *et al.* 2013) to vary as $\epsilon \approx 22u'^{3.5}$ m^2 s^{-3} under the same operating conditions. All droplets fell many times their stopping distance before reaching the isotropic region. Within this region, most travelled $O(10^1–10^2)$ times their stopping distance before being measured. Droplets with $d > 150$ µm did not travel their stopping distance and were excluded to avoid the possibility that this might affect the results. Experiments were performed for three flow conditions, labelled E1, E2 and E3. Table 1 summarizes the flow parameters for each, while the diagonal lines in figure 2 indicate the ranges of particle parameters in each experiment. Unlike for the DNS, gravity was fixed and so different Froude numbers were achieved by slight adjustments in R_λ.
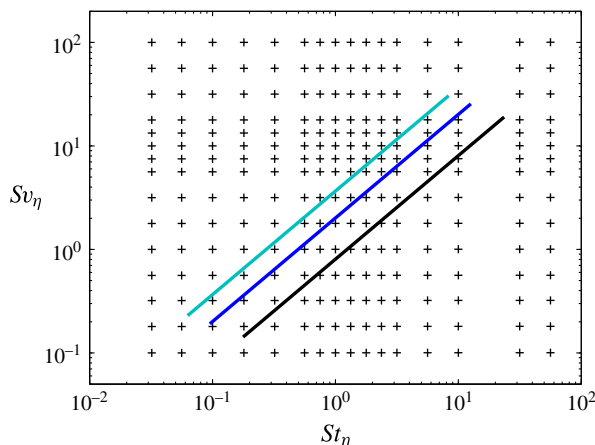
FIGURE 2. The investigated particle groups. The crosses represent the DNS and the light and dark blue and black lines represent E1, E2 and E3, respectively.

2.3. *Direct numerical simulations*

We performed DNS of isotropic (box) turbulence using a pseudospectral code to solve the three-dimensional incompressible Navier–Stokes equations in a tri-periodic cube of length $\mathscr{L} = 2\pi$ (Ireland *et al.* 2013). Statistical stationarity of the fluid field was achieved through a deterministic large-scale forcing scheme (Witkowska, Brasseur & Juvé 1997). Once stationarity of the particle fields was reached, their statistics were averaged over at least 10 τ_ℓ. Three simulations were performed, labelled S1, S2 and S3, in order of increasing Reynolds number. The turbulence parameters are provided in table 1.

For the particle field, we assumed one-way coupling and used the simplified momentum equation $d_t u_p = (u - u_p)/(\tau_p/f_D) + g$ (Tchen 1947). Five hundred and thirteen independent particle classes were simulated simultaneously, each denoted in figure 2, apart from the $g = 0$ groups. The particle parameters were set by independently changing τ_p and g (fixing $\rho_p/\rho = 877$). In this way, multiple Froude numbers were investigated at fixed Reynolds numbers, allowing us to decouple the role of each. Two particle fields were simulated for every particle class, one with linear Stokes drag ($f_D = 1$) and one with the nonlinear drag model, $f_D = 1 + 0.15R_p^{0.687}$ (Clift, Grace & Weber 1978), where $R_p \equiv |u - u_p|\, d/\nu$ is the instantaneous particle Reynolds number and d is calculated from τ_p. One concern with fast-falling particles is that they could be influenced by the periodic boundary conditions (e.g. Woittiez, Jonker & Portela 2009). For S2 and S3, this problem is anticipated for particles with $Sv_\ell \gtrsim 5$. Results from S1 (which has better large-scale resolution and is therefore safe up to $Sv_\ell \approx 13$) suggest that the qualitative trends in the particle settling and r.m.s. velocities are unaffected by the domain periodicity.

3. Results

3.1. *Settling regimes*

We define the turbulent settling speed difference as $(W - W_o)/u'$, which takes on a positive value for turbulence-enhanced settling and a negative value for turbulence-inhibited settling. Figure 3(*a*) shows the results for all experiments and
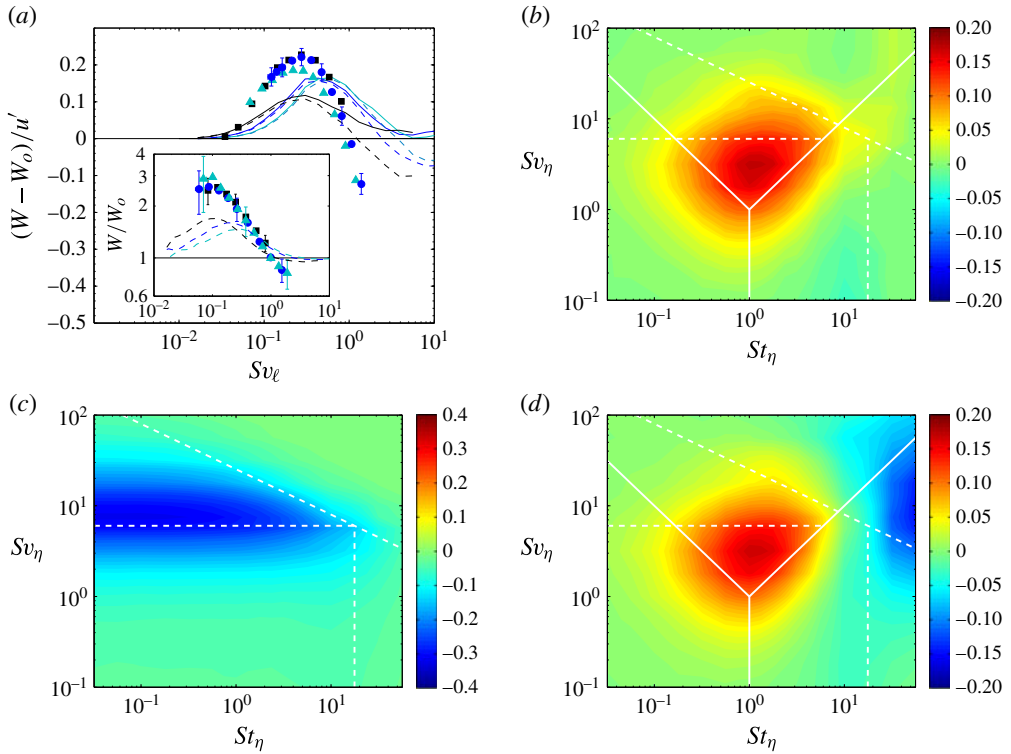
759 R3-5

FIGURE 3. (a) $(W - W_o)/u'$ for experiments E1, E2 and E3 with light blue, dark blue and black symbols. The inset shows W/W_o, also as a function of Sv_ℓ. Sample error bars are shown, which in the main plot omit an ordinate error of $\pm 0.05u'$ due to the mean flow speed uncertainty in each experiment. The solid (linear drag) and dashed (nonlinear drag) lines of matching colour show S2 data interpolated to the same Fr. (b) Isocontours of $(W - W_o)/u'$ on the St_η–Sv_η plane for the S2 data with linear drag, (c) linear drag with the particles confined to vertical paths and (d) nonlinear drag. The solid white lines show unity St_η, $Fr/a_o^{1/2}$ (+1 slope) and $Sv_\eta St_\eta$ (−1 slope); the dashed white lines show unity St_ℓ, Sv_ℓ and $St_\ell Sv_\ell^2$ ($\frac{-1}{2}$ slope).

for S2 with both drag models as a function of Sv_ℓ in order to address the settling bifurcation discussed in §1. There is clear experimental evidence of both enhanced and reduced settling velocities. For small values of Sv_ℓ, the settling velocities are enhanced by turbulence, while at larger values of Sv_ℓ, the settling velocities are reduced. This reduction should reach a maximum and the settling speed should return to the still-fluid value as $Sv_\ell \to \infty$ (Nielsen 1993; Kawanisi & Shiozaki 2008); however, this trend is not apparent in the data, most likely due to the limited range of particles that could be measured in this experiment. On the other hand, the DNS do appear to plateau to a minimum value, while the measurements continue a downward trend, with both showing settling reductions up to $(W - W_o)/u' \approx -0.1$. In their works, Nielsen (1993) and Kawanisi & Shiozaki (2008) examined a different scaling for the reductions, W/W_o. We show this scaling in the inset to figure 3(a). The measurements for W/W_o show a tendency to an inflection point consistent with that in Kawanisi & Shiozaki (2008), although measurements at higher Sv_ℓ are needed.

These appear to be the first experiments to clearly demonstrate both the enhanced and the reduced settling regimes for particles with $\rho_p/\rho \sim 1000$. (As noted earlier, the Good *et al.* (2012) data, which showed these trends, were shifted by a non-zero mean flow.) Qualitatively similar results have been obtained considering particles with density ratios $\rho_p/\rho < 10$ in aqueous turbulence (Murray 1970; Nielsen 1993; Srdic 1998; Kawanisi & Shiozaki 2008).

The experimental results in figure 3(*a*) confirm the qualitative arguments set forth by Nielsen (1993). The DNS data allow us to further analyse these arguments. The DNS with linear drag are in qualitative agreement with the experiments for lower values of Sv_ℓ; they, however, show no evidence of loitering at higher Sv_ℓ. To confirm this point, figure 3(*b*) shows isocontours of $(W - W_o)/u'$ over the entire simulated range of parameters with linear drag. Consistent with earlier DNS performed over narrower parameter ranges (Wang & Maxey 1993; Yang & Lei 1998; Ireland & Collins 2012), $(W - W_o)/u' > 0$ for all conditions. The qualitative disagreement between experiments and DNS has been an open question in the literature. Nielsen (1993) argued that fast-falling particles ($Sv_\ell \gtrsim 1$) should bisect the eddies and 'loiter' in the upward flows, causing $(W - W_o)/u' < 0$. In an effort to reproduce loitering with linear drag, we performed a DNS in which particles were artificially confined to vertical paths (i.e. the horizontal velocities were set to zero). The results of this artificial flow are shown in figure 3(*c*). Despite the absence of any nonlinear drag effects, the settling velocities are reduced and the reduction clearly depends on Sv_ℓ, validating Nielsen's arguments. The reduction peaks for order-one Sv_ℓ, with a value of $(W - W_o) \lesssim -0.4u'$ in this artificial case. It is difficult to say to what extent the loitering bias competes with the fast-tracking bias in real turbulence, where particles are not artificially confined to vertical paths. Contrasting figures 3(*b*) and (*c*), we conclude that with linear drag, the bias caused by preferential sampling exceeds that of loitering, resulting in $(W - W_o)/u' > 0$ over the entire parameter plane.

Reduced settling speeds in DNS have only been observed either by artificially eliminating lateral movement (cf. figure 3*c*) or by introducing a nonlinear drag law (see the dashed lines in figures 3*a*,*d*). The explanation is that nonlinear drag can facilitate a loitering bias for certain particle classes. It should be noted that a simple drag coefficient cannot capture all the nonlinear effects in a time-dependent flow like turbulence and thus the experimental and DNS data are in considerable quantitative disagreement, particularly at large Sv_ℓ. A more rigorous approach would be to perform a particle-resolved DNS (e.g. see Uhlmann 2008; Lucci, Ferrante & Elghobashi 2010). The recent particle-resolved simulations of Garcia-Villalba, Kidanemariam & Uhlmann (2012) in fact showed nonlinear drag to play a leading role where there are fluctuating drag forces. Nevertheless, based on all the evidence, we conclude that the simplistic treatment of the nonlinearities is sufficient to reach the qualitative conclusion that the reduced settling speeds at higher Stokes numbers result from nonlinear drag effects.

We now focus on various scaling relationships proposed in the literature. We highlight that in certain regions of the figure 3 contour plots the gradients indicate that the settling trends chiefly change with a single parameter that may differ from the simpler and more traditional scalings of the Stokes or settling numbers. These features are instructive as to which characteristics, such as the inertial response time, Stokes velocity or particle stopping distance, govern the behaviour of different particle classes. The results also highlight the important scales of the flow.

For particles with low St_η and low Sv_η (i.e. weak inertia and gravity), Bec, Homann & Ray (2014) showed that by relating particle settling velocities to clustering in planes perpendicular to gravity (see also Gustavsson, Vajedi & Mehlig 2014), the settling

speed difference $(W - W_o)/u' \propto St_\eta Sv_\eta$ (analogous to the 'transit time' Stokes number, $\tau_p/(\eta/\tau_p g)$, proposed by Dávila & Hunt 2001). The scaling $(W - W_o)/u' \propto St_\eta Sv_\eta$ agrees well with the trends in the DNS for weak gravity and inertia. We also note that some contours of both the enhanced and the reduced settling regimes seem to be parallel to lines of constant $Fr \propto St_\eta Sv_\eta^{-1} \propto g^{-1}$, indicating that $(W - W_o)/u'$ is independent of the particle size or response time there. This result has not yet been reported, and we are unsure of its physical or theoretical explanation.

Dávila & Hunt (2001) obtained the scaling $St_\ell Sv_\ell^2$ by considering the motion of heavy particles around a two-dimensional steady vortex. They referred to this as the particle Froude number, which represents the ratio of the particle stopping distance to the typical path length around an eddy. In figures 3(b,c), the particles are unable to have biased trajectories for large St_ℓ or $St_\ell Sv_\ell^2$ with linear drag. For S2 in figure 3(d), the enhanced and reduced settling regions are separated by the $St_\ell = 1$ line. For S1, however, there is less scale separation, the regions are closer together and the settling reductions extend to $St_\ell < 1$, where they are instead separated by the $St_\ell Sv_\ell^2 = 1$ line. When figure 3(a) is plotted as a function of $St_\ell Sv_\ell^2$, the measurements are qualitatively similar, with the transition to turbulence-reduced settling also appearing to occur for $St_\ell Sv_\ell^2 \gtrsim 1$. Although not conclusive, these trends are all consistent with the arguments of Dávila & Hunt (2001) and Ghosh *et al.* (2005). We do note for the experiments, however, that $u'^2/\ell g \sim O(1)$ and thus that droplets with order-one Sv_ℓ coincidentally also have nearly order-one $St_\ell Sv_\ell^2$, and vice versa.

Regarding figure 3(d), the S1 and S3 trends ($R_\lambda = 105$ and 227) are qualitatively the same as those shown for S2 ($R_\lambda = 140$). For small St_η and Sv_η, the results match in the St_η–Sv_η plane. At large values, the picture stretches with R_λ and the bounds of the enhanced and reduced settling regions simply move in the St_η–Sv_η plane with the dashed white lines that show the critical large-scale parameters. This demonstrates how the behaviour is governed by the small-scale parameters where they are small and by the large-scale parameters where they are large.

3.2. *Particle fluctuating velocities*

In this section, we discuss the fluctuations in the particle velocities as a function of the system parameters. As noted by Salazar & Collins (2012), the particle r.m.s. velocity can exceed the fluid r.m.s. velocity at low Stokes numbers and negligible gravity as a result of biased sampling induced by particle inertia (i.e. the particles preferentially sample the more energetic regions of the fluid). However, this quickly gives way to filtering effects that generally cause u'_p/u' to be a decreasing function of the particle Stokes number.

Wang & Stock (1993) analysed the effects due to filtering and derived algebraic models for the dependence of w'_p and v'_p on inertial and gravitational parameters (see their equations (2.24) and (2.25)). From this we obtain expressions for the particle velocity r.m.s. and its anisotropy. For strong gravitational effects ($Sv_\ell \gg 1$), the equations essentially reduce to functions of $St_\ell Sv_\ell$. For weak gravity, u'_p/u' becomes a function of St_ℓ and the anisotropy v'_p/w'_p asymptotes to a function of Sv_ℓ for $St_\ell \to \infty$.

We test this model against the u'_p/u' measurements and DNS in figure 4(a). The experimental and DNS data each collapse well as functions of $St_\ell Sv_\ell$ for the Froude numbers of the experiments (see figure 2) (for which $u'_p \approx u'$ for $Sv_\ell < 1$). The S2 data and experiments are both in qualitative agreement with the model. Figure 4(b) shows isocontours of the ratio u'_p/u' on the St_ℓ–Sv_ℓ plane taken from S1 (due to its better statistics and large-scale resolution, although no qualitative difference from the
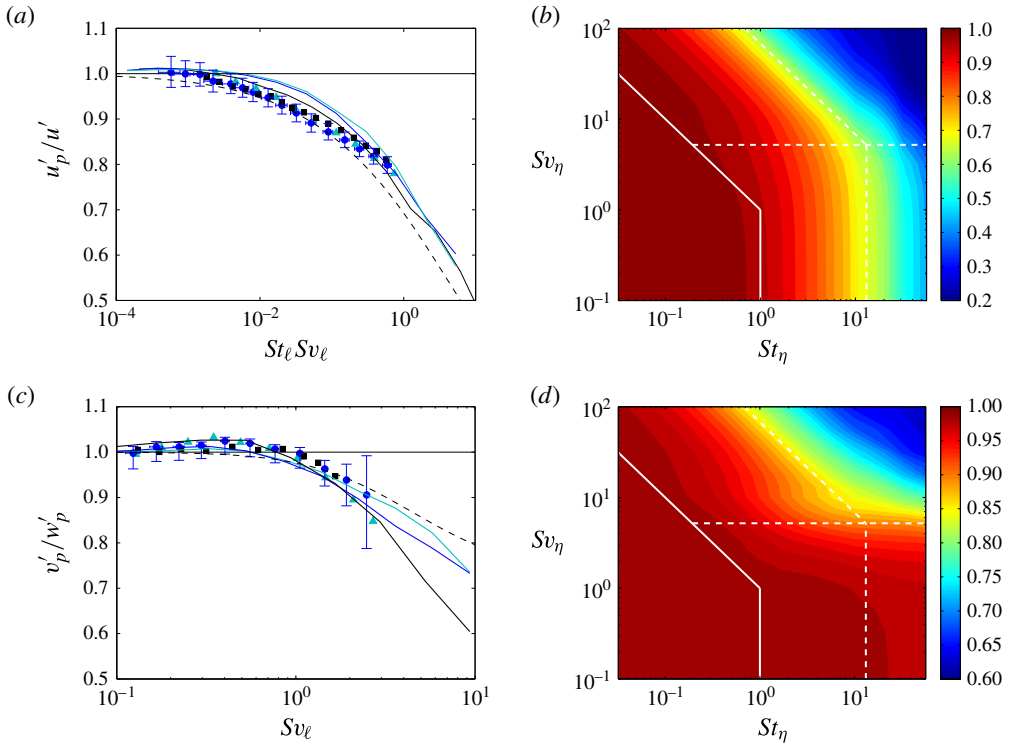
FIGURE 4. Comparison between the experiment, DNS and theory for (*a*) u'_p/u' and (*c*) v'_p/w'_p. The symbols show E1 (light blue), E2 (dark blue) and E3 (black) with sample error bars for E2. The solid lines of matching colour show S2 (nonlinear drag) data at the same Froude numbers; the black dashed lines show the theoretical prediction from Wang & Stock (1993) calculated with the help of their equation (2.30) for the S2 turbulence with $Fr = 0.9$. Also shown are S1 (linear drag) isocontours of (*b*) u'_p/u' and (*d*) v'_p/w'_p. The solid white lines show unity St_η and $St_\eta Sv_\eta$ (−1 slope), while the dashed white lines show unity St_ℓ, Sv_ℓ and $St_\ell Sv_\ell$ (−1 slope).

other R_λ or drag cases was seen). The results confirm that when gravitational forces are strong, the isocontours of u'_p/u' are parallel to lines of constant $St_\ell Sv_\ell$. For $Sv_\ell < 1$, the critical parameter is St_ℓ, in agreement with Wang & Stock (1993) and Salazar & Collins (2012).

In figure 4(*c*), we see that the theoretical prediction for the particle motion anisotropy agrees well with the experiments and DNS data as functions of Sv_ℓ. The v'_p/w'_p isocontour slopes in figure 4(*d*) reflect both the Sv_ℓ and $St_\ell Sv_\ell$ scalings of the Wang & Stock (1993) model discussed above, with the slight discrepancy at small Sv_ℓ probably due to noise. In all cases, the particles' vertical velocity fluctuations are greater than or equal to their horizontal ones, since vertically falling particles have more time to respond to the vertical fluctuations of the turbulence, as the longitudinal integral scale is twice the transverse one (Yudine 1959; Csanady 1963; Wang & Stock 1993). The DNS are in reasonable agreement with the $v'_p/w'_p \to \sqrt{1/2} \approx 0.7$ limit of the model for the largest values of St_ℓ and Sv_ℓ, and the slight discrepancies are probably due to noise, periodicity effects or the slight anisotropy in the underlying turbulence. Finally, we note that regions of strong anisotropy seem to coincide with

regions of settling velocity reduction. The physical explanation is that particles are unable to side-step turbulent eddies and therefore cannot fast-track when horizontal particle velocity fluctuations are weak.

4. Conclusions

Using experiments and DNS, we have examined the settling regimes of heavy inertial particles in a turbulent flow. While the experiments indicate that reduced settling speeds are present for certain particle classes, DNS data over a wide range of inertia and gravitational forces show no such settling velocity reductions when the particles are subjected to linear drag forces, and settling velocity reductions in DNS are only possible when a nonlinear drag correction is introduced. While the DNS with nonlinear drag is able to capture the qualitative trends in the experiment, quantitative differences highlight the need for studies using particle-resolved DNS.

Since the DNS results showed no settling velocity reductions with linear drag, we introduced an artificial test case where we confined particles to vertical paths and assumed linear drag forces in an attempt to reproduce the 'loitering effect' discussed in Nielsen (1993). We observed reduced settling velocities in this case, providing evidence for the loitering effect in this artificial flow. Apparently, with only linear drag forces, the effects of preferential sweeping dominate the loitering effect, resulting in enhancements to the settling velocity in *all* conditions.

Our results show that the settling velocity depends sensitively on both particle inertia and the settling parameter. While the settling velocity may be governed by a single parameter in certain limits (e.g. $St_\eta Sv_\eta$ in the limit of tracer particles in $Fr > 1$ flows), the general settling behaviour is more complex and depends on the scales of both the smallest and the largest eddies of the turbulence, the ratios of which (e.g. ℓ/η or u'/u_η) are to first order determined by R_λ.

We then analysed the r.m.s. particle velocity and r.m.s. particle velocity anisotropy to better understand the dynamics of heavy inertial particles. For moderate and large St_η or $St_\eta Sv_\eta$, the r.m.s. particle velocities decreased with increasing inertia and gravity. For weak gravitational effects, the dominant parameter affecting the particle velocity fluctuations was the particle Stokes number, in agreement with Wang & Stock (1993) and Salazar & Collins (2012). For strong gravitational effects ($Sv_\ell \gg 1$), the r.m.s. particle velocities were seen to be generally dependent on $St_\ell Sv_\ell$, in agreement with Wang & Stock (1993), and the experimental, DNS and theoretical results matched well.

The velocity r.m.s. anisotropy is always such that vertically falling particles respond more to vertical than to horizontal fluctuations, the physical explanation being that the vertical fluctuations are correlated over longer vertical distances than the horizontal ones. We showed that the model of Wang & Stock (1993) is in good agreement with the experimental measurements and DNS data. We also observed that regions of high velocity r.m.s. anisotropy generally coincided with regions of settling velocity reductions, suggesting that fast-tracking vanishes when particles have a diminished response to horizontal velocity fluctuations. In anisotropic flows, the ratio of the longitudinal and transverse integral scales can grow like nearly the cube of the velocity r.m.s. anisotropy (Bewley, Chang & Bodenschatz 2012). This points to the possibility of anisotropy having interesting effects on the settling behaviour in addition to the effects of the coherent shear structures or inhomogeneous (i.e. transient) conditions falling particles may also encounter in real flows.

Acknowledgements

References

ALISEDA, A., CARTELLIER, A., HAINAUX, F. & LASHERAS, J. C. 2002 Effect of preferential concentration on the settling velocity of heavy particles in homogeneous isotropic turbulence. *J. Fluid Mech.* **468**, 77–105.

BEC, J., HOMANN, H. & RAY, S. S. 2014 Gravity-driven enhancement of heavy particle clustering in turbulent flow. *Phys. Rev. Lett.* **112**, 184501.

BEWLEY, G. P., CHANG, K. & BODENSCHATZ, E. 2012 On integral length scales in anisotropic turbulence. *Phys. Fluids* **24**, 061702.

BEWLEY, G. P., SAW, E. W. & BODENSCHATZ, E. 2013 Observation of the sling effect. *New J. Phys.* **15**, 083051.

BOSSE, T. & KLEISER, L. 2006 Small particles in homogeneous turbulence: settling velocity enhancement by two-way coupling. *Phys. Fluids* **18**, 027102.

CHANG, K., BEWLEY, G. P. & BODENSCHATZ, E. 2012 Experimental study of the influence of anisotropy on the inertial scales of turbulence. *J. Fluid Mech.* **692**, 464–481.

CLIFT, R., GRACE, J. R. & WEBER, M. E. 1978 *Bubbles, Drops, and Particles*. Academic Press.

CSANADY, G. T. 1963 Turbulent diffusion of heavy particles in the atmosphere. *J. Atmos. Sci.* **20**, 201–208.

DÁVILA, J. & HUNT, J. C. R. 2001 Settling of small particles near vortices and in turbulence. *J. Fluid Mech.* **440**, 117–145.

ELGHOBASHI, S. & TRUESDELL, G. C. 1993 On the two-way interaction between homogeneous turbulence and dispersed solid particles. I: turbulence modification. *Phys. Fluids* A **5**, 1790–1801.

GARCIA-VILLALBA, M., KIDANEMARIAM, A. G. & UHLMANN, M. 2012 DNS of vertical plane channel flow with finite-size particles: Voronoi analysis, acceleration statistics and particle-conditioned averaging. *Intl J. Multiphase Flow* **46**, 54–74.

GHOSH, S., DÁVILA, J., HUNT, J. C. R., SRDIC, A., FERNANDO, H. H. S. & JONAS, P. R. 2005 How turbulence enhances coalescence of settling particles with applications to rain in clouds. *Proc. R. Soc. Lond.* A **461**, 3059–3088.

GOOD, G. H., GERASHCHENKO, S. & WARHAFT, Z. 2012 Intermittency and inertial particle entrainment at a turbulent interface: the effect of the large-scale eddies. *J. Fluid Mech.* **694**, 371–398.

GUSTAVSSON, K., VAJEDI, S. & MEHLIG, B. 2014 Clustering of particles falling in a turbulent flow. *Phys. Rev. Lett.* **112**, 214501.

HILL, R. J. 2005 Geometric collision rates and trajectories of cloud droplets falling into a Burgers vortex. *Phys. Fluids* **17**, 037103.

IRELAND, P. J. & COLLINS, L. R. 2012 Direct numerical simulation of inertial particle entrainment in a shearless mixing layer. *J. Fluid Mech.* **704**, 301–332.

IRELAND, P. J., VAITHIANATHAN, T., SUKHESWALLA, P. S., RAY, B. & COLLINS, L. R. 2013 Highly parallel particle-laden flow solver for turbulence research. *Comput. Fluids* **76**, 170–177.

KAWANISI, K. & SHIOZAKI, R. 2008 Turbulent effects on the settling velocity of suspended sediment. *J. Hydraul. Engng* **134** (2), 261–266.

KELLEY, D. H. & OUELLETTE, N. T. 2011 Using particle tracking to measure flow instabilities in an undergraduate laboratory experiment. *Am. J. Phys.* **79**, 267–273.

LUCCI, F., FERRANTE, A. & ELGHOBASHI, S. 2010 Modulation of isotropic turbulence by particles of Taylor length-scale size. *J. Fluid Mech.* **650**, 5–55.

MAXEY, M. R. 1987 The gravitational settling of aerosol particles in homogeneous turbulence and random flow fields. *J. Fluid Mech.* **174**, 441–465.

MURRAY, S. P. 1970 Settling velocities and vertical diffusion of particles in turbulent water. *J. Geophys. Res.* **75**, 1647–1654.

NIELSEN, P. 1993 Turbulence effects on the settling of suspended particles. *J. Sedim. Petrol.* **63** (5), 835–838.

SALAZAR, J. P. L. C. & COLLINS, L. R. 2012 Inertial particle relative velocity statistics in homogeneous isotropic turbulence. *J. Fluid Mech.* **696**, 45–66.

SAWFORD, B. L., YEUNG, P. K., BORGAS, M. S., VEDULA, P., PORTA, A. LA, CRAWFORD, A. M. & BODENSCHATZ, E. 2003 Conditional and unconditional acceleration statistics in turbulence. *Phys. Fluids* **15** (11), 3478–3489.

SRDIC, A. 1998 PhD thesis, Arizona State University.

SUNDARAM, S. & COLLINS, L. R. 1999 A numerical study of the modulation of isotropic turbulence by suspended particles. *J. Fluid Mech.* **379**, 105–143.

TCHEN, C. M. 1947 PhD thesis, Technische Hogeschool Delft.

TOOBY, P. F., GERALD, L. W. & JOHN, D. I. 1977 The motion of a small sphere in a rotating velocity field: a possible mechanism for suspending particles in turbulence. *J. Geophys. Res.* **82** (15), 2096–2100.

UHLMANN, M. 2008 Interface-resolved direct numerical simulation of vertical particulate channel flow in the turbulent regime. *Phys. Fluids* **20**, 053305.

WANG, L. P. & MAXEY, M. R. 1993 Settling velocity and concentration distribution of heavy particles in homogeneous isotropic turbulence. *J. Fluid Mech.* **256**, 26–68.

WANG, L.-P. & STOCK, D. E. 1993 Dispersion of heavy particles by turbulent motion. *J. Atmos. Sci.* **50**, 1897–1913.

WITKOWSKA, A., BRASSEUR, J. G. & JUVÉ, D. 1997 Numerical study of noise from isotropic turbulence. *J. Comput. Acoust.* **5**, 317–336.

WOITTIEZ, E. J. P., JONKER, H. J. J. & PORTELA, L. M. 2009 On the combined effects of turbulence and gravity on droplet collisions in clouds: a numerical study. *J. Atmos. Sci.* **66**, 1926–1943.

YANG, C. Y. & LEI, U. 1998 The role of turbulent scales in the settling velocity of heavy particles in homogeneous isotropic turbulence. *J. Fluid Mech.* **371**, 179–205.

YANG, T. S. & SHY, S. S. 2003 The settling velocity of heavy particles in an aqueous near-isotropic turbulence. *Phys. Fluids* **15**, 868–880.

YANG, T. S. & SHY, S. S. 2005 Two-way interaction between solid particles and homogeneous air turbulence: particle settling rate and turbulence modification measurements. *J. Fluid Mech.* **526**, 171–216.

YUDINE, M. I. 1959 Physical considerations of heavy-particle diffusion. *Adv. Geophys.* **6**, 185–191.